IEEE Access
Multidisciplinary ⋮ Rapid Review ⋮ Open Access Journal

Received 5 April 2024, accepted 17 April 2024, date of publication 29 April 2024, date of current version 24 May 2024.

Digital Object Identifier 10.1109/ACCESS.2024.3394843

RESEARCH ARTICLE

Comparing Hybrid Approaches of Deep Learning for Remaining Useful Life Prognostic of Lithium-Ion Batteries

ANAS TIANE[1], (Member, IEEE), CHAFIK OKAR[1,2], (Member, IEEE), MOHAMAD ALZAYED[1], (Member, IEEE), AND HICHAM CHAOUI[1], (Senior Member, IEEE)

[1]Intelligent Robotic and Energy Systems Research Group (IRES), Department of Electronics, Carleton University, Ottawa, ON K1S 5B6, Canada
[2]National School of Applied Sciences of Tetouan, Abdelmalek Essaâdi University, Tetouan 93000, Morocco

Corresponding author: Mohamad Alzayed (mohamad.alzayed@carleton.ca)

ABSTRACT Many published journals used hybrid deep learning methods to predict batteries' remaining useful life by adopting different rationales to select and combine deep learning methods aiming to propose the most accurate prediction model possible. The main contribution of this article consists of proposing, to the best of the authors' knowledge, the most accurate hybrid deep learning prediction model, designed and configured by considering the theoretical strength of each of the selected deep learning models, combined with meticulous data preprocessing and feature engineering steps. A benchmark study is presented to confirm the theoretical design by comparing the prediction results of the selected hybrid model with other proposed hybrid deep learning algorithms. The selected prediction model is compared as well with previously published articles, specifically, the ones that have used hybrid deep learning methods, NASA datasets, and batteries #6, #7, and #18 selectively. The hybrid model refers to the combination of different types of deep learning architectures, such as Convolutional Neural Networks (CNNs), Deep Neural Networks (DNN), Long Short-Term Memory (LSTM), Bidirectional Long Short-Term Memory (bLSTM), recurrent neural network (RNN), Bidirectional recurrent neural network (bRNN), Gated recurrent units (GRU) and Bidirectional Gated recurrent units (bGRU). This combination includes CNN-LSTM-DNN, CNN-bLSTM-DNN, CNN-GRU-DNN, CNN-bGRU-DNN, CNN-RNN-DNN, and CNN-bRNN-DNN, and aims to leverage the strengths of each architecture in capturing spatial, temporal, and sequential patterns present in the battery dataset. The hybrid deep learning approaches are tested with multichannel inputs, encompassing parameters such as voltage, current, and temperature, as well as their respective time series averages. The objective is to predict the remaining useful life. Performance evaluation is conducted using error metrics, including Mean Absolute Error (MAE) and Root Mean Square Error (RMSE). The results revealed a remarkable 90.5% enhancement in RMSE, indicating substantial improvement.

INDEX TERMS Lithium-ion battery, remaining useful life, deep neural network, machine learning.

LIST OF ABBREVIATIONS

ANN	Artificial neural network.
AUKF	Adaptive unscented Kalman filter.
BSA	Backtracking spiral algorithm.
CALCE	Center for advanced life cycle engineering.
CNN	Convolutional neural network.
DAE	Denoising autoencoders.
DBNN	Deep belief neural network.
DL	Deep learning.
DNN	Deep neural network.
EEMD	Ensemble empirical mode decomposition.
ELM	Extreme learning machine.
FFNN	Feed forward neural network.
FOS	Forgetting online sequential.
FOSELM	Forgetting online sequential extreme learning.
GPR	Gaussian process regression.

The associate editor coordinating the review of this manuscript and approving it for publication was Alberto Cano.

GRU	Gated recurrent units.
HGWO	Hybrid grey wolf optimizer.
HKA	Heuristic Kalman algorithm.
IS	Importance sampling.
LSTM	Long short-term memory.
MAE	Mean absolute error.
ML	Machine learning.
MLP	Multi-layer perceptron.
MLR	Multiscale logistic regression.
NASA	National aeronautics and space administration.
PF	Particle filter.
PSO	Particle swarm optimization.
PSR	Phase space reconstruction.
RMSE	Root mean square error.
RNN	Recurrent neural network.
RVM	Relevance vector machine.
SRU	Simple recurrent units.
SVM	Support vector machines.
SVR	Support vector regression.

I. INTRODUCTION

The increasing environmental instability, encompassing factors like carbon emissions, climate change, and global warming, along with heightened fuel consumption, prompted the development of robust energy storage and management systems. Among these systems, batteries—such as lead-acid, lithium-ion, Ni-MH, and Ni-Cd batteries—stand out as crucial and efficient forms of energy storage [1]. They serve as primary power sources across diverse domains, including electric vehicles, space systems, consumer electronics, aerospace electronics, and mobile communications [2]. Nonetheless, the longevity of batteries gradually diminishes due to internal electrochemical reactions, physical and chemical alterations within the cells, as well as external factors like temperature variations and discharge rates [3], [4]. The repercussions of battery failure encompass compromised performance, disruptions in device functionality, increased maintenance expenses, financial losses, and potential safety hazards [5]. Hence, accurately forecasting the lifespan of Li-ion batteries becomes imperative to ensure reliability, safety, and optimal battery performance [6].

The Remaining Useful Life (RUL) of a battery refers to the number of remaining charge-discharge cycles before it reaches a critical failure point, typically around 70–80% of its original capacity [7]. Estimating the RUL can be achieved through four main methods: direct measurement, model-based approaches, data-driven techniques, and hybrid methods [8]. Direct measurement methods involve assessing the battery's capacity and impedance using parameters like open-circuit voltage and Electrochemical Impedance Spectroscopy. Model-based approaches utilize various models such as electrochemical, equivalent circuits, or empirical models, often incorporating filtering algorithms like Kalman filter, unscented Kalman filter, or particle filter. Data-driven prediction methods, including Artificial Neural Networks (ANN), Support Vector Machines (SVM), and Relevance Vector Machines (RVM), leverage historical battery data features such as capacity, current, voltage, temperature, and impedance to forecast RUL without the need for an in-depth understanding of the system. Among these methods, neural networks have been extensively employed for predicting the RUL of Li-ion batteries due to their superior learning capabilities compared to traditional algorithms [31].

Hybrid methods combine both data-driven and model-based techniques or solely rely on data-driven approaches to forecast the RUL of Li-ion batteries. Thanks to advancements in Machine Learning (ML) and Deep Learning (DL), coupled with improved computational hardware and accessible datasets like those from NASA and CALCE, researchers have been able to explore and implement such algorithms effectively for accurate RUL prediction.

Numerous studies have leveraged hybrid neural network approaches for estimating RUL in Li-ion batteries. For instance, Xia et al. [9] introduced a method comprising Feedforward Neural Network (FFNN) and Importance Sampling (IS), demonstrating robust RUL prediction. Li et al. and Yang et al. utilized two methods, MPSO-ELM [10] and HKA-ELM [11], with the latter enhancing the stochastic parameters of the Extreme Learning Machine (ELM) algorithm to improve predictability. Ren et al. [12] proposed an integrated deep learning approach combining an Autoencoder model with a Deep Neural Network for enhanced prediction accuracy. Jia et al. [13] introduced a novel prognostic method, the Multi-layer Perceptron Particle Filter (MLP-PF). Zraibi et al. [14] combined the Particle Filter (PF) algorithm with Artificial Neural Network (ANN) for RUL estimation. Fan et al. [15] proposed a deep learning method integrating the Forgetting Online Sequential Extreme Learning Machine (FOS-ELM) with the Hybrid Grey Wolf Optimizer (HGWO) algorithm. Zhu et al. [16] incorporated Differential Evolution (DE) into their hybrid method named DGWO-ELM, improving prediction accuracy and performance. Dong et al. [17] introduced a Neural Network (NN) method for modeling battery degradation based on the bat-based particle filter. Wang et al. [18] proposed a new RUL prediction method combining Ensemble Empirical Mode Decomposition (EEMD) and Nonlinear Autoregressive (NAR) neural network models, achieving high prediction accuracy. Zhang et al. [19] combined Partial Incremental Capacity and ANN for RUL battery prediction. Wang et al. [20] presented a hybrid neural network method named Elman-Long Short-Term Memory (LSTM) for RUL estimation, merging the empirical model decomposition algorithm with LSTM and Elman neural networks. Ansari et al. [3] utilized a hybrid NN method named Convolutional Neural Network (CNN)-LSTM, which reduced errors and increased accuracy. Chen et al. [21] introduced the hybrid method ELM-BSASVM, which outperformed individual methods.

TABLE 1. Rul estimation results of some other papers.

Articles	Battery	Algorithms	RMSE	MAE
[29]	B6	MLR-GPR		0.0609
[11]	B6	ELM		
		PSO-ELM		
		MPSO-ELM		
	B18	ELM		
		PSO-ELM		
		MPSO-ELM		
[15]	B6	RNN	0.1131	
		LSTM	0.1216	
		RVM	0.0784	
		HA-FOSELM	0.0434	
	B7	RNN	0.1132	
		LSTM	0.0284	
		RVM	0.1138	
		HA-FOSELM	0.1021	
[12]	B7	ADNN	0.0666	
[19]	B6	IC-ANN	0.0533	0.0341
	B7	IC-ANN	0.0511	0.0325
	B18	IC-ANN	0.0401	0.0279
[18]	B6	EEMD-NARNN	0.0520	
	B7	EEMD-NARNN	0.0483	
[33]	B7	SVR	0.0441	
		PSO-SVR	0.0223	
		QPSO-SVR	0.0185	
[28]	B6	UKF	0.0617	0.0465
		AUKF	0.0527	0.0395
		AUKF-GASVR	0.0510	0.0392
	B7	UKF	0.0658	0.0446
		AUKF	0.0142	0.0094
		AUKF-GASVR	0.0134	0.0091
	B18	UKF	0.0666	0.0450
		AUKF	0.0556	0.0388
		AUKF-GASVR	0.0547	0.0382
[5]	B6	RVM	0.0667	
		GM	0.0634	
		RVM-GM	0.0306	
	B7	RVM	0.0272	
		GM	0.0248	
		RVM-GM	0.0119	
	B18	RVM	0.0227	
		GM	0.0266	
		RVM-GM	0.0101	
[31]	B6	MC-RNN	0.0339	0.0272
		MC-GRU	0.0271	0.0180
		MC-SRU	0.0504	0.0478
		MC-LSTM	0.0152	0.0103
	B7	MC-RNN	0.0204	0.0184

TABLE 1. *(continued.)* Rul estimation results of some other papers.

Articles	Battery	Algorithms	RMSE	MAE
		MC-GRU	0.0200	0.0186
		MC-SRU	0.0163	0.0126
		MC-LSTM	0.0085	0.0068
	B18	MC-RNN	0.0369	0.0304
		MC-GRU	0.0433	0.0294
		MC-SRU	0.0585	0.0427
		MC-LSTM	0.0388	0.0261
[30]	B6	PSR-GASVR	0.0634	
		PSR-GASVR-EC	0.0081	
	B7	PSR-GASVR	0.0927	
		PSR-GASVR-EC	0.0101	
	B18	PSR-GASVR	0.0765	
		PSR-GASVR-EC	0.0051	
[16]	B6	PF-SVR	0.0248	
		DGWO-ELM	0.0097	
	B7	PF-SVR	0.0147	
		DGWO-ELM	0.0043	

In contrast, non-deep learning hybrid algorithms may rely on more conventional machine learning techniques like regression or ensemble methods such as random forests. They may also incorporate techniques like improved variational modal decomposition (VMD), particle filter (PF), and Gaussian process regression (GPR). While these methods have been widely employed and can yield satisfactory results in specific contexts, they may require extensive feature engineering and lack the ability to automatically learn intricate patterns from raw data.

To conduct a rigorous benchmark study, this article concentrates on comparing its predictions with studies that have utilized hybrid methods, specifically with NASA datasets, and have targeted batteries #6, #7, and #18. Studies [5], [15], [28], [29], [31] employed hybrid methods combining two algorithms, aligning with the approach adopted in this article. Additionally, studies [16] and [30] utilized hybrid methods combining three algorithms, mirroring the number of combined algorithms utilized in this article. This focus ensures a comprehensive and relevant comparison of prediction performance within the context of hybrid methods and specific battery selections from the NASA dataset.

Table 1 presents a summary of RUL prediction results arranged from the least favorable to the most favorable outcomes. It is evident that [16] and [30] exhibit superior performance compared to [5], [15], [28], [29], and [31]. However, it is noteworthy that the proposed hybrid algorithm surpasses all others in terms of predictive accuracy and effectiveness.

The primary contributions of this study can be outlined as follows:

1- Conducting a comprehensive comparative analysis between existing hybrid deep learning algorithms and novel hybrid learning algorithms, which integrate various neural network (NN) architectures such as CNN-LSTM-DNN, CNN-bLSTM-DNN, CNN-GRU-DNN, CNN-bGRU-DNN, CNN-RNN-DNN, and CNN-bRNN-DNN. These hybrid algorithms are meticulously designed and sequenced based on the unique strengths of each constituent learning algorithm. It is noteworthy that these proposed hybrid algorithms have not been previously explored. The comparison is specifically tailored to articles focusing on predicting batteries' remaining useful life using hybrid deep learning algorithms, leveraging selectively the NASA datasets pertaining to batteries #6, #7, and #18.

2- Introducing a novel feature engineering methodology that has proven to be highly effective for any feature sequence represented in the format of time series data. The study demonstrates the impact of employing this feature engineering approach versus not incorporating it, providing valuable insights into its efficacy.

3- Evaluating the performance of the proposed method by comparing its results with state-of-the-art approaches, particularly those utilizing three combined algorithms akin to this study. The findings highlight substantial performance enhancements achieved by the proposed hybrid methods. These improvements are quantitatively assessed using performance indicators such as Mean Absolute Error (MAE) and Root Mean Squared Error (RMSE) on NASA datasets. Notably, the proposed method demonstrates a notable reduction in error rates and a significant increase in accuracy.

In summary, the motivation behind the adoption of hybrid models stems from their ability to leverage the complementary strengths inherent in diverse deep-learning architectures. By amalgamating multiple deep learning models within a hybrid framework, researchers can effectively capitalize on the full spectrum of these techniques, thereby addressing the intricate challenges posed by real-world datasets, including the prediction of battery life. This approach enables improved prediction accuracy and generalization compared to individual models, ultimately facilitating the resolution of complex tasks such as battery life prediction.

The other sections of this paper are prepared as follows: Section II explains the architecture of proposed hybrid methods. Section III explains the RUL estimation method used in this article. Section IV explains the data preprocessing and feature engineering methods. Section V lists the proposed method results. Finally, a conclusion is given.

II. PROPOSED DEEP LEARNING HYBRID METHODS

Two learning methodologies are generally used in ML and DL methods, namely supervised and unsupervised learning. Supervised learning methods depend on target features to train and learn over the feature datasets, whereas unsupervised methods do not depend on it. Supervised learning methods are used to resolve regression and classification problems. Another advantage of DL, compared to ML methods, is that DL algorithms abstract the manual feature extraction step by automatically selecting relevant features. DL architecture is more complex than ML and has more hidden layers than ANN [22].

Recently, various DL methods based on time series prediction were shown in several works, e.g., DAE, DBNN, CNN, RNN, LSTM, and GRU. This paper focuses its study on eight variants of DL, i.e., CNN, DNN, RNN, LSTM, GRU, bRNN, bLSTM, and bGRU.

CNN is competent in feature extraction and very fast in training compared to standard sequence modeling. CNN shows two important advantages, i.e., local dependency and scale invariance. Its method of feature extraction takes a hierarchical form. Its architecture contains convolutional, pooling, fully connected layers, and output layers. The first layer extracts different features of input through the convolution process containing several feature planes and neurons. The second layer is secondary feature extraction; it reduces the feature surface dimension and its resolution for obtaining constant spatial features. The convolution and pooling layers are mapped one to one, each to another, where the outputs of the convolution layer are the inputs of the pooling layer. The third layer can combine the information from the previous layers. The final layer receives full connection outputs [35].

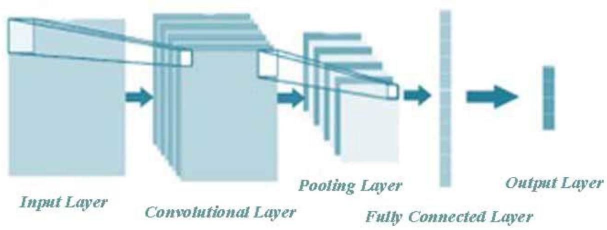

FIGURE 1. The architecture of the CNN.

RNN is one of the most popular algorithms among DL methods. It leverages the temporal correlations between neurons, and RNN is used to treat tasks that include the sequence of the features. It also has internal memory to remember past results and to discover the best way to make the next best estimation. However, RNN experiences problems with long-distance dependencies that contribute to gradient vanishing symptoms where the gradient tends to 0 and, therefore, does not contribute to forward learning. To overcome the RNN gradient vanishing issue, two variants of RNN are used, i.e. LSTM and GRU, to control the propagation of gradient information and remember the parameters as subsequent inputs during the long-term sequence [19]. GRU uses two gates: the first is called update gate (z), which controls the hidden state update, and the second gate is called reset gate (r), which decides if it should ignore the previous hidden state or not [23]. LSTM architecture contains three gates, i.e. the input (i), forget (f) and output (o), as well as a memory unit [24]. It is obvious that GRU has a simpler architecture and fewer gates compared to LSTM by combining the forget and output gates of LSTM in one gate, namely the update gate. LSTM's equations can be defined as follows:

$$
\begin{aligned}
f_t &= \sigma(W_f\,[h_{t-1}, x_t] + b_f) \\
\mathrm{i_t} &= \sigma(W_i\,[h_{t-1}, x_t] + b_i) \\
o_t &= \sigma(W_o\,[h_{t-1}, x_t] + b_o \\
q_t &= \tanh(W_q\,[h_{t-1}, x_t] + b_q) \\
c_t &= f_t * c_{t-1} + i_t * q_t \\
h_t &= o_t * \tanh(c_t)
\end{aligned} \tag{1}
$$

The previous and the current cell states are identified respectively as q and c, the unit output as (h), the weight matrices, the bias, and the sigmoid function represented as W, b, and σ, [24]. GRU's equations can be defined as follows:

$$
\begin{aligned}
z_t &= \sigma(W_z\,[h_{t-1}, x_t]) \\
\mathrm{r_t} &= \sigma(W_r\,[h_{t-1}, x_t]) \\
\tilde{h}_t &= \tanh(W_h\left[r_t * h_{t-1}, x_t\right]) \\
h_t &= ((1 - z_t) * h_{t-1}) + (z_t * \tilde{h}_t)
\end{aligned} \tag{2}
$$

where, $\tilde{h}_t$ is the candidate gate and h_t is output activation [23].

The single algorithms described so far process the previous data only, while the bidirectional algorithms as bRNN [25], bLSTM [26], and bGRU [27] have the ability to process the data inputs in both directions, i.e., the forward and backward temporal sequences, allowing these bidirectional algorithms to be more efficient is defining the relationship between the sequences and its model.

To leverage the advantages of each algorithm and enhance the RUL prediction accuracy, a hybrid formula is proposed in this article, integrating CNN, RNN, LSTM, bLSTM, GRU, bGRU/ and DNN. The DL technology uses multiple layers to extract higher-level features from the raw input progressively.

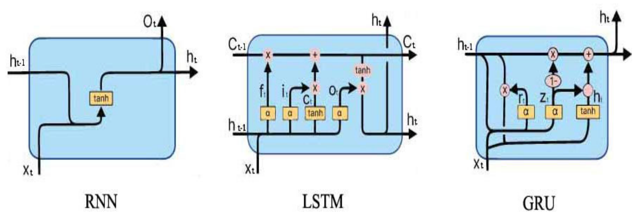

FIGURE 2. The architecture of each the RNN, LSTM, and GRU.

In the presented work, CNN is applied to extract local features, capture the spatial relationship, and use shared weights' structure to reduce the amount of the weights and try to find the shared information from the measurement of data. One convolutional layer is used with 160 filters, including the kernel of size 4. The configuration used one default stride, causal padding, and Relu activation function. The RNN / LSTM/ bRNN / bLSTM/ GRU/ bGRU were applied to understand the temporal relationships within the feature sequence by using their internal state (memory) to learn features and time dependencies from the sequential data and capture temporal features. Each of these algorithms had two layers consisting of 160 nodes followed by a flattened layer. Finally, DNN has been used to map the features by choosing 4 dense layers, each of them containing a Relu activation function with 160 nodes. A dense layer with one node is used as a regression layer to get the final RUL output.

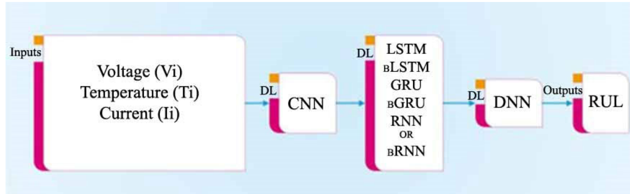

FIGURE 3. The architecture of the proposed hybrid methods.

III. RUL ESTIMATION

The estimation method of accurate capacity is an essential prerequisite in order to successfully predict the RUL since the degradation process of the battery is affected by a series of factors like temperature (T), current (I), voltage (V) and capacity (C), the more parameters included in the process, the higher model accuracy can be achieved.

This paper proposes six hybrid methods of deep learning time series for RUL prediction of lithium-ion batteries with multichannel inputs, where the inputs are Vn, In, Tn, and the average sequence of the previous time steps of these features (i.e. I2500avg, V2500avg, T2500avg), ranging from 0 to 2500 time steps. The proposed method's output is the target RUL. The final model is constructed by combining some basic neural networks, namely CNN, LSTM, DNN, and GRU, as follows: CNN-LSTM-DNN, CNN-bLSTM-DNN, CNN-GRU-DNN, CNN-bGRU-DNN, CNN-RNN-DNN and CNN-bRNN-DNN. Noted CLD, CbLD, CGD, CbGd, CRD, and CbRD.

A. SYSTEM CONFIGURATION AND EVALUATION CRITERIA OF PERFORMANCE

The proposed hybrid algorithms were tested using a Server with Intel(R) Xeon(R) CPU ES-2687W 3.10GHz with two processors and 256 GB of memory. Tensorflow 2.0 has been used to implement these algorithms using the Anaconda 3.0 library. Adam optimizer and Huber loss function were used as a rectified linear unit (ReLU) activation function.

The performance of RUL prediction of the algorithms was assessed using the mean absolute error [2] and root mean square error [28], denoted as MAE and RMSE, respectively. Their mathematical equations are defined as follows:

$$MAE = \sum\nolimits_{k=1}^{k} |y_k - \widehat{y_k}| \tag{3}$$

$$RMSE = \sqrt{\frac{1}{N}\sum_{i=1}^{N}(y_k - \widehat{y_k})^2} \tag{4}$$

where, y_k, $\widehat{y_k}$, and indicates the true value and the estimated value of actual battery capacity. The best prediction accuracy is achieved when the error value is close to zero for MAE and RMSE.

RUL is defined as the remaining number of cycles (charge/discharge) to get to the failure threshold of the battery with a specific output capacity [36], (i.e., the length of time from the current time to the end of life "EOL"). The EOL is considered as the time when the capacity gets to 70–80% of the nominal capacity [36], [37]. It can be written as:

$$\mathrm{RUL} = \mathrm{T_{EOL}} - \mathrm{T_{cc}} \tag{5}$$

$\mathrm{T_{cc}}$ is the cycle number of current capacity and $\mathrm{T_{EOL}}$ is the cycle number when the capacity reaches the EOL threshold [3].

IV. DATA PREPROCESSING AND FEATURE ENGINEERING

A. NASA DATASETS

Data used in this paper has been acquired from NASA [32]. From all available data sets representing Li-ion battery readings, three data sets were chosen representing three batteries (model number 18650): B0006, B0007 and B0018 as shown in Fig. 4.

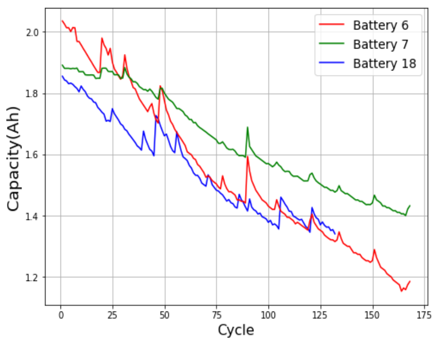

FIGURE 4. Capacity degradation curve of NASA batteries.

The issue of limited data availability in NASA datasets is indeed a challenge that must be carefully addressed when employing deep learning techniques. In response to this concern, several strategies are explored to mitigate the impact of limited data on model performance, such as data augmentation techniques to increase the size and diversity of the dataset artificially and investigating the effectiveness of transfer learning approaches, where pre-trained models on larger datasets are fine-tuned on the specific NASA dataset of interest.

Batteries are examined at room temperature, 24 degrees Celsius, during three different operational processes (i.e., charge, discharge, and impedance). Table 2 lists some technical characteristics of the selected batteries.

TABLE 2. The description of nasa batteries.

Constant charge current	1.5A
Minimal charge current	20mA
Discharge current	2A
nominal capacity	2Ah
Charge/Discharge cut-off voltage	4.2/2.5V
charge/discharge cycles	168 (B6,B7) and 137 (B18)

B. DATA PREPARATION

Three data modes were available in the NASA data set:

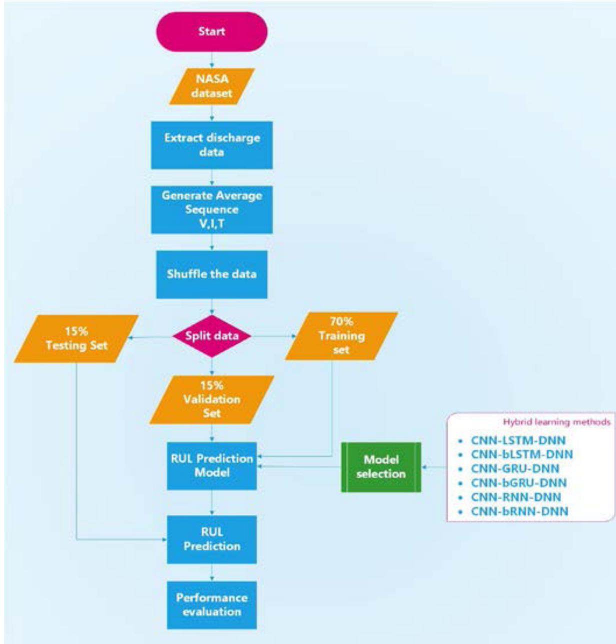

FIGURE 5. Data preparation.

The charging mode experiment is first charged with a constant current (CC) of 1.5A until the voltage is 4.2V, then in a constant voltage (CV) until the current drops to 20mA. The discharge mode process was discharged with a constant current (CC) of 2A until the voltage was decreased to 2.5V of B0006. When the measured actual capacity mode of the Li-ion battery became lower than 70% of the rated capacity (2Ah), the experiment stopped.

As shown in Fig. 5, the first step was to extract the discharge data, generate the average sequence as explained in the feature engineering section, and then shuffle and split it as follows: 70% as training data, 15% for validation and 15% for testing.

C. FEATURE ENGINEERING

The feature engineering step consists of selecting features that are fed to the algorithms. Two RUL prediction results for battery #6 are compared in this section using two feature engineering methods. The first method constructs for each feature, i.e. V, I and T, a simple time-series sequence using the last 13 values plus the capacity as follows:

Simple Time-Series Set:

- $(v_1, v_2, v_3, v_4, v_5, v_6, v_7, v_8, v_9, v_{10}, v_{11}, v_{12}, v_{13})$
- $(t_1, t_2, t_3, t_4, t_5, t_6, t_7, t_8, t_9, t_{10}, t_{11}, t_{12}, t_{13})$
- $(\mathrm{i}_1, \mathrm{i}_2, i_3, i_4, i_5, i_6, i_7, i_8, i_9, i_{10}, i_{11}, i_{12}, i_{13})$

The second sequence is represented with a floating average time series using a window size of 200 starting from reading 2500. The sequence is represented as follows:

Average Time-Series Set:

- $(v_{avr2500}, v_{avrg2300}, v_{avrg2100}, v_{avrg1900}, v_{avrg1700}, v_{avrg1500}, v_{avrg1300}, v_{avrg1100}, v_{avrg900}, v_{avrg700}, v_{avrg500}, v_{avrg300}, v_{avrg100})$
- $(t_{avrg2500}, t_{avrg2300}, t_{avrg2100}, t_{avrg1900}, t_{avrg1700},$

CNN LSTM DNN

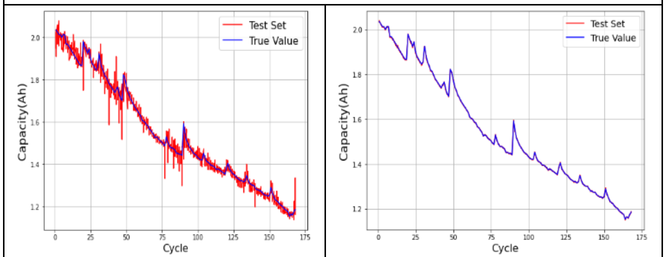

Prediction using simple sequence | Prediction using average sequence

	MAE	RMSE
Average sequence	0.00069	0.00097
Simple sequence	0.00862	0.01459
Improvement	91.99%	93.35%

CNN bLSTM DNN

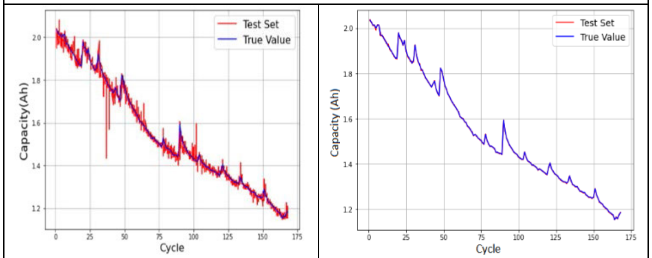

Prediction using simple sequence | Prediction using average sequence

	MAE	RMSE
Average sequence	0.00055	0.00077
Simple sequence	0.01328	0.00739
Improvement	95.86%	89.58%

CNN GRU DNN

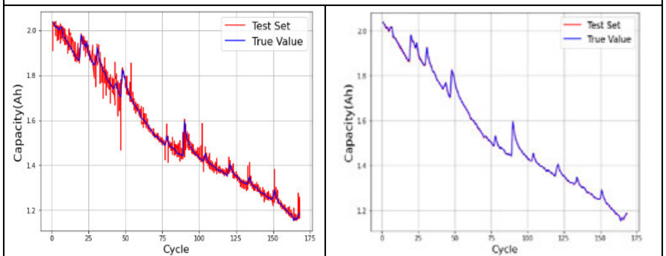

Prediction using simple sequence | Prediction using average sequence

	MAE	RMSE
Average sequence	0.00144	0.00211
Simple sequence	0.00819	0.01383
Improvement	82.41%	84.74%

CNN bGRU DNN

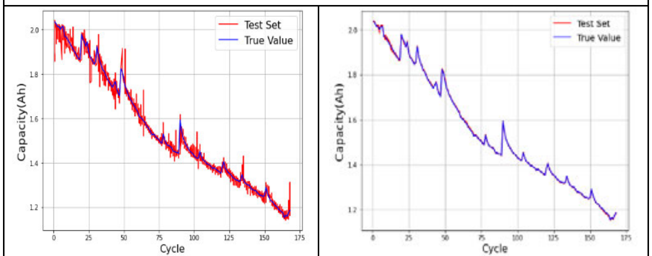

Prediction using simple sequence | Prediction using average sequence

	MAE	RMSE
Average sequence	0.00059	0.00084
Simple sequence	0.00821	0.01394
Improvement	92.81%	93.97%

CNN RNN DNN

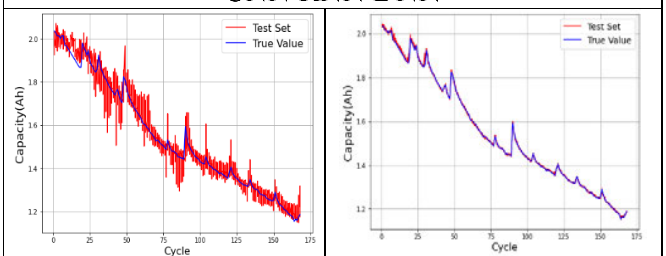

Prediction using simple sequence | Prediction using average sequence

	MAE	RMSE
Average sequence	0.00254	0.00395
Simple sequence	0.02221	0.03116
Improvement	88.56%	87.32%

CNN bRNN DNN

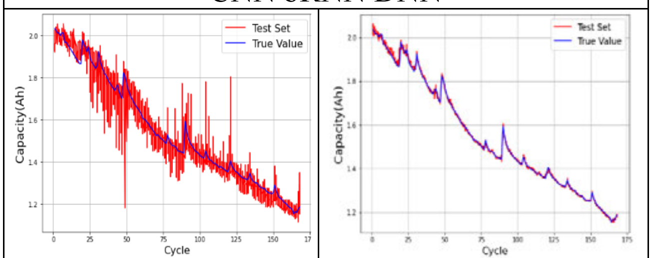

Prediction using simple sequence | Prediction using average sequence

	MAE	RMSE
Average sequence	0.00372	0.00559
Simple sequence	0.02776	0.04033
Improvement	86.56%	86.13%

FIGURE 6. Results of RUL prediction comparison for B0006 using an average and simple sequence.

$t_{avrg1500}, t_{avrg1300}, t_{avrg1100}, t_{avrg900}, t_{avrg700}, t_{avrg500}, t_{avrg300}, t_{avrg100}$

- $(\mathrm{i}_{avrg2500}, \mathrm{i}_{avrg2300}, \mathrm{i}_{avrg2100}, \mathrm{i}_{avrg1900}, \mathrm{i}_{avrg1700}, \mathrm{i}_{avrg1500}, \mathrm{i}_{avrg1300}, \mathrm{i}_{avrg1100}, \mathrm{i}_{avrg900}, \mathrm{i}_{avrg700}, \mathrm{i}_{avrg500}, \mathrm{i}_{avrg300}, \mathrm{i}_{avrg100}$

The following figures compare results for RUL predictions for battery #6 using the six hybrid algorithms in two scenarios. The first scenario uses the simple time-series sequence, and the second uses the average time-series sequence. True values and test dataset curves are represented by blue and red colors, respectively. Prediction results, as shown in Fig. 6, show a prediction improvement of at least 82.41% between the two featuring methods.

V. VALIDATION AND DISCUSSION

This section presents, analyses and compares the RUL prediction of Li-ion batteries using six different hybrid methods.

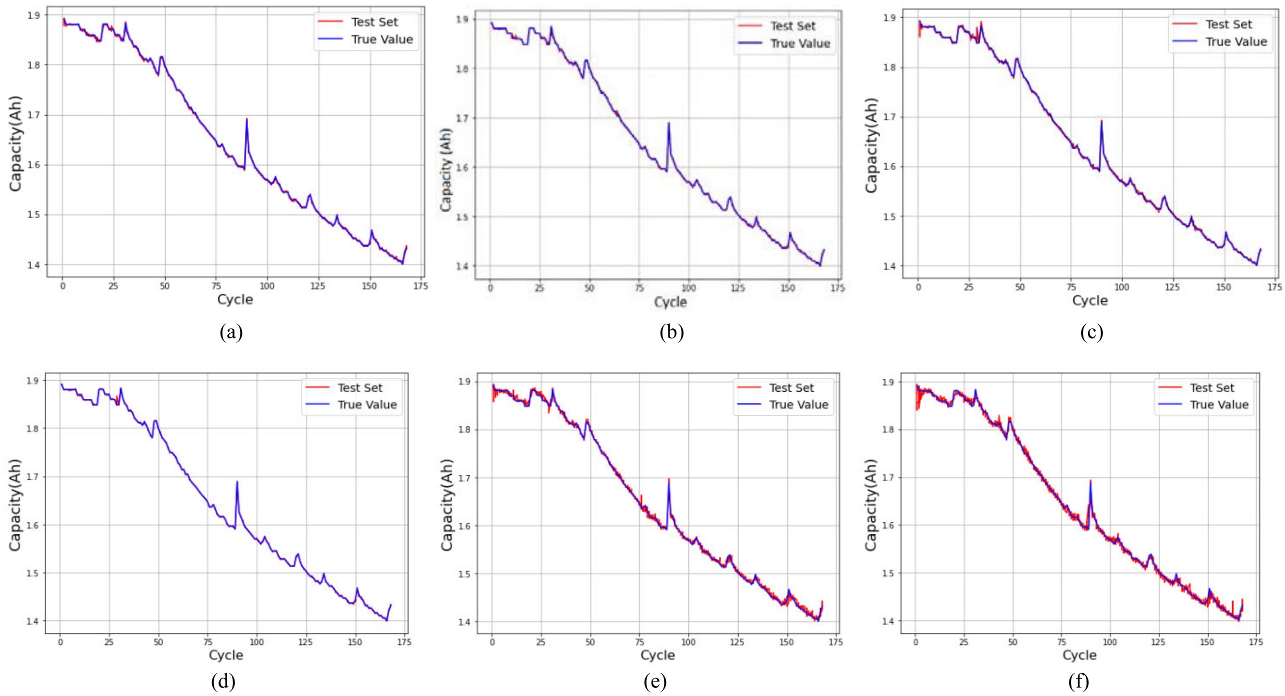

FIGURE 7. Results of RUL prediction for B0007 using: (a) CLD., (b) CbLD, (c) CGD, (d) CbGD, (e) CRD, and (f) CbRD.

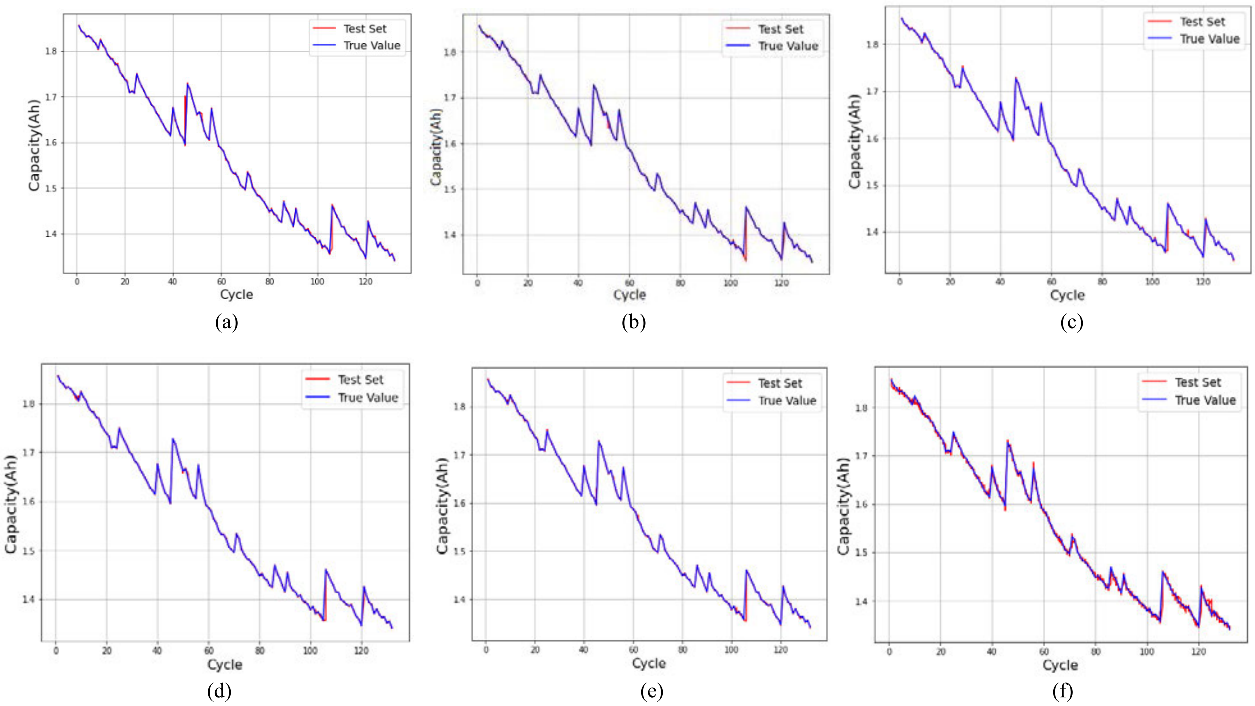

FIGURE 8. Results of RUL prediction for B0018 using: (a) CLD., (b) CbLD, (c) CGD, (d) CbGD, (e) CRD, and (f) CbRD.

In addition, it introduces a comparative analysis of the RUL prediction between the proposed methods and the best methods in other papers.

Fig. 7 and 8 show the results of the six proposed hybrid methods to predict the RUL of the B7 and B18 Li-ion batteries.

Table 3 and 4 list RUL prediction results of Li-ion batteries using six different hybrid methods sorted in ascending order (from best to worst prediction results) as shown in Fig. 6, 7, and 8.

Overall, CbLD and CbGD are deemed to show the best prediction results. To put these numbers in perspective, they are compared to the best RUL prediction results available in the literature. The comparison is limited to articles listed in Table 1. The commonality between articles selected for the benchmark is that they all use hybrid methods to predict

TABLE 3. MAE RUL estimation results for NASA batteries, ascendant order.

MAE					
B6		B7		B18	
CbLD	0.00055	CbLD	0.00034	CbGD	0.00032
CbGD	0.00059	CbGD	0.00035	CbLD	0.00033
CLD	0.00069	CLD	0.00087	CRD	0.00035
CGD	0.00144	CGD	0.0009	CGD	0.0004
CRD	0.00254	CRD	0.00239	CLD	0.00071
CbRD	0.00372	CbRD	0.00302	CbRD	0.00269

TABLE 4. RMSE RUL estimation results for NASA batteries, ascendant order.

RMSE					
B6		B7		B18	
CbLD	0.00077	CbGD	0.00052	CGD	0.00156
CbGD	0.00084	CbLD	0.00057	CbGD	0.00158
CLD	0.00097	CLD	0.00116	CRD	0.00163
CGD	0.00211	CGD	0.00131	CbLD	0.00182
CRD	0.00395	CRD	0.0033	CLD	0.00216
CbRD	0.00559	CbRD	0.00452	CbRD	0.00384

TABLE 5. RMSE improvement.

Battery	Algorithm	RMSE	RMSE Improvement
B6	CbLD	0.00077	90.49%
	PSR-GASVR-EC [30]	0.0081	
B7	CbGD	0.00052	87.91%
	DGWO-ELM [16]	0.0043	
B18	CGD	0.00156	69.41%
	PSR-GASVR-EC [30]	0.0051	

batteries' RUL; they all use NASA datasets and specifically consider batteries #6, #7 and #18. More specifically, the benchmark focus on two articles [16] and [30] for two reasons:

1/ Table 1 is sorted in descending order, and RUL prediction is listed from worst to best. Therefore, [16] and [30] show the best battery RUL prediction so far in the available literature.

2/ [16] and [30] combine three algorithms in their hybrid configuration, just like this article.

Therefore, the benchmark is legitimate. RMSE is used to compare the results. The best RUL prediction results for each battery is selected amongst all algorithms.

Table 5 shows that the RMSE improvement is significant and that the proposed algorithms overclass the ones used so far in the literature. Overall, the performance of different approaches depends on a combination of factors including model complexity, feature representation, data quality, hyperparameter tuning, assumptions, robustness, and computational efficiency. Understanding these factors can help practitioners select the most appropriate approach for their specific task and dataset.

VI. CONCLUSION

This paper presents the RUL prediction of Li-ion batteries aiming to improve the prediction accuracy using six different hybrid deep learning methods CNN-LSTM-DNN, CNN-BLSTM-DNN, CNN-GRU-DNN, CNN-BGRU-DNN, CNN-RNN-DNN, and CNN-BRNN-DNN. The proposed hybrid methods were experimentally validated on datasets obtained from NASA and their performance, which demonstrate a high RUL prediction accuracy assessed by the RMSE, MAE. Finally, a benchmark study proved that the accuracy reached in this article outclass any other previously published works of literature covering the same subject, knowingly, RUL prediction of Li-ion batteries using NASA datasets, specifically batteries #6, #7 and #18. Future iterations of the research plan may consider expanding the scope of deep learning methods to encompass a wider array of architectures, including the Transformers method, to ensure a more comprehensive evaluation of state-of-the-art techniques. The findings of this study are constrained by specific datasets, necessitating validation of hybrid models across diverse datasets, while future research should streamline model complexity without compromising accuracy, enhance interpretability of deep learning-based RUL estimation models, and address data availability and quality challenges through techniques like data augmentation and anomaly detection.

REFERENCES

[1] A. Singh, K. Pal, and C. B. Vishwakarma, "State of charge estimation techniques of Li-ion battery of electric vehicles," *e-Prime-Adv. Electr. Eng., Electron. Energy*, vol. 6, Dec. 2023, Art. no. 100328, doi: 10.1016/j.prime.2023.100328.

[2] M. Arrinda, M. Oyarbide, H. Macicior, and E. Muxika, "Unified evaluation framework for stochastic algorithms applied to remaining useful life prognosis problems," *Batteries*, vol. 7, no. 2, p. 35, May 2021, doi: 10.3390/batteries7020035.

[3] G. Ma, Y. Zhang, C. Cheng, B. Zhou, P. Hu, and Y. Yuan, "Remaining useful life prediction of lithium-ion batteries based on false nearest neighbors and a hybrid neural network," *Appl. Energy*, vol. 253, Nov. 2019, Art. no. 113626, doi: 10.1016/j.apenergy.2019.113626.

[4] C. C. Liu, T. Wu, and C. He, "State of health prediction of medical lithium batteries based on multi-scale decomposition and deep learning," *Adv. Mech. Eng.*, vol. 12, no. 5, May 2020, Art. no. 168781402092320, doi: 10.1177/1687814020923202.

[5] L. Zhao, Y. Wang, and J. Cheng, "A hybrid method for remaining useful life estimation of lithium-ion battery with regeneration phenomena," *Appl. Sci.*, vol. 9, no. 9, p. 1890, May 2019, doi: 10.3390/app9091890.

[6] T.-H. Kim, J.-H. Cho, Y.-K. Kim, and J.-H. Chang, "Deep-learning-based prediction algorithm for fuel cell electric vehicle energy with shift mixup," *IEEE Sensors J.*, early access, Mar. 11, 2024, doi: 10.1109/JSEN.2024.3373078.

[7] J. Xu, A. Zhen, Z. Cai, P. Wang, K. Gao, and D. Jiang, "State of health diagnosis and remaining useful life prediction of lithium-ion batteries based on multi-feature data and mechanism fusion," *IEEE Access*, vol. 9, pp. 85431–85441, 2021, doi: 10.1109/ACCESS.2021.3083395.

[8] B. Gou, Y. Xu, and X. Feng, "State-of-health estimation and remaining-useful-life prediction for lithium-ion battery using a hybrid data-driven method," *IEEE Trans. Veh. Technol.*, vol. 69, no. 10, pp. 10854–10867, Oct. 2020, doi: 10.1109/TVT.2020.3014932.

[9] X. Xia, J. Yue, Y. Guo, C. Lv, X. Zeng, Y. Xia, and G. Chen, "Technologies for energy storage power stations safety operation: Battery state evaluation survey and a critical analysis," *IEEE Access*, vol. 12, pp. 31334–31356, 2024, doi: 10.1109/ACCESS.2024.3370847.

[10] L. Li, Z. Huang, and G. Ding, "Indirect prediction for lithium-ion batteries RUL using multi-objective arithmetic optimization algorithm-based deep extreme learning machine," *IEEE Access*, vol. 11, pp. 110400–110416, 2023, doi: 10.1109/ACCESS.2023.3320058.

[11] J. Yang, Z. Peng, Z. Pei, Y. Guan, H. Yuan, and L. Wu, "Remaining useful life assessment of lithium-ion battery based on HKA-ELM algorithm," *Int. J. Electrochem. Sci.*, vol. 13, no. 10, pp. 9257–9272, Oct. 2018, doi: 10.20964/2018.10.51.

[12] L. Ren, L. Zhao, S. Hong, S. Zhao, H. Wang, and L. Zhang, "Remaining useful life prediction for lithium-ion battery: A deep learning approach," *IEEE Access*, vol. 6, pp. 50587–50598, 2018, doi: 10.1109/ACCESS.2018.2858856.

[13] X. Jia, C. Zhang, L. Y. Wang, L. Zhang, and X. Zhou, "Early diagnosis of accelerated aging for lithium-ion batteries with an integrated framework of aging mechanisms and data-driven methods," *IEEE Trans. Transport. Electrific.*, vol. 8, no. 4, pp. 4722–4742, Dec. 2022, doi: 10.1109/TTE.2022.3180805.

[14] B. Zraibi, C. Okar, H. Chaoui, and M. Mansouri, "Remaining useful life assessment for lithium-ion batteries using CNN-LSTM-DNN hybrid method," *IEEE Trans. Veh. Technol.*, vol. 70, no. 5, pp. 4252–4261, May 2021, doi: 10.1109/TVT.2021.3071622.

[15] J. Fan, J. Fan, F. Liu, J. Qu, and R. Li, "A novel machine learning method based approach for Li-ion battery prognostic and health management," *IEEE Access*, vol. 7, pp. 160043–160061, 2019, doi: 10.1109/ACCESS.2019.2947843.

[16] J. Zhu, T. Tan, L. Wu, and H. Yuan, "RUL prediction of lithium-ion battery based on improved DGWO-ELM method in a random discharge rates environment," *IEEE Access*, vol. 7, pp. 125176–125187, 2019, doi: 10.1109/ACCESS.2019.2936822.

[17] H. Dong, "Prediction of the remaining useful life of lithium-ion batteries based on Dempster–Shafer theory and the support vector regression-particle filter," *IEEE Access*, vol. 9, pp. 165490–165503, 2021, doi: 10.1109/ACCESS.2021.3136131.

[18] P. Wang, X. Dan, and Y. Yang, "A multi-scale fusion prediction method for lithium-ion battery capacity based on ensemble empirical mode decomposition and nonlinear autoregressive neural networks," *Int. J. Distrib. Sensor Netw.*, vol. 15, no. 3, Mar. 2019, Art. no. 155014771983963, doi: 10.1177/1550147719839637.

[19] S. Zhang, B. Zhai, X. Guo, K. Wang, N. Peng, and X. Zhang, "Synchronous estimation of state of health and remaining useful lifetime for lithium-ion battery using the incremental capacity and artificial neural networks," *J. Energy Storage*, vol. 26, Dec. 2019, Art. no. 100951, doi: 10.1016/j.est.2019.100951.

[20] Y. Wang, C. Hei, H. Liu, S. Zhang, and J. Wang, "Prognostics of remaining useful life for lithium-ion batteries based on hybrid approach of linear pattern extraction and nonlinear relationship mining," *IEEE Trans. Power Electron.*, vol. 38, no. 1, pp. 1054–1063, Jan. 2023, doi: 10.1109/TPEL.2022.3182135.

[21] X. D. Chen, H. Y. Yang, J. S. Wun, C. H. Wang, and L. L. Li, "Life prediction of lithium-ion battery based on a hybrid model," *Energy Explor. Exploitation*, vol. 38, no. 5, pp. 1854–1878, Sep. 2020, doi: 10.1177/0144598720911724.

[22] P. K. Das, D. V. A, S. Meher, R. Panda, and A. Abraham, "A systematic review on recent advancements in deep and machine learning based detection and classification of acute lymphoblastic leukemia," *IEEE Access*, vol. 10, pp. 81741–81763, 2022, doi: 10.1109/ACCESS.2022.3196037.

[23] M. Sajjad, Z. A. Khan, A. Ullah, T. Hussain, W. Ullah, M. Y. Lee, and S. W. Baik, "A novel CNN-GRU-based hybrid approach for short-term residential load forecasting," *IEEE Access*, vol. 8, pp. 143759–143768, 2020, doi: 10.1109/access.2020.3009537.

[24] L. Chaudhary, N. Girdhar, D. Sharma, J. Andreu-Perez, A. Doucet, and M. Renz, "A review of deep learning models for Twitter sentiment analysis: Challenges and opportunities," *IEEE Trans. Computat. Social Syst.*, pp. 1–30, 2023, doi: 10.1109/TCSS.2023.3322002.

[25] M. C. Gursesli, S. Lombardi, M. Duradoni, L. Bocchi, A. Guazzini, and A. Lanata, "Facial emotion recognition (FER) through custom lightweight CNN model: Performance evaluation in public datasets," *IEEE Access*, vol. 12, pp. 45543–45559, 2024, doi: 10.1109/access.2024.3380847.

[26] Z. Wei, Q. Zhu, C. Min, Y. Chen, and G. Wang, "Bidirectional hybrid LSTM based recurrent neural network for multi-view stereo," *IEEE Trans. Vis. Comput. Graphics*, p. 1, 2022, doi: 10.1109/TVCG.2022.3165860.

[27] K. Zhang, Y. Cai, Y. Ren, R. Ye, and L. He, "MTF-CRNN: Multiscale time-frequency convolutional recurrent neural network for sound event detection," *IEEE Access*, vol. 8, pp. 147337–147348, 2020, doi: 10.1109/ACCESS.2020.3015047.

[28] Z. Xue, Y. Zhang, C. Cheng, and G. Ma, "Remaining useful life prediction of lithium-ion batteries with adaptive unscented Kalman filter and optimized support vector regression," *Neurocomputing*, vol. 376, pp. 95–102, Feb. 2020, doi: 10.1016/j.neucom.2019.09.074.

[29] J. Jia, J. Liang, Y. Shi, J. Wen, X. Pang, and J. Zeng, "SOH and RUL prediction of lithium-ion batteries based on Gaussian process regression with indirect health indicators," *Energies*, vol. 13, no. 2, p. 375, Jan. 2020, doi: 10.3390/en13020375.

[30] L. Chen, Y. Zhang, Y. Zheng, X. Li, and X. Zheng, "Remaining useful life prediction of lithium-ion battery with optimal input sequence selection and error compensation," *Neurocomputing*, vol. 414, pp. 245–254, Nov. 2020, doi: 10.1016/j.neucom.2020.07.081.

[31] K. Park, Y. Choi, W. J. Choi, H.-Y. Ryu, and H. Kim, "LSTM-based battery remaining useful life prediction with multi-channel charging profiles," *IEEE Access*, vol. 8, pp. 20786–20798, 2020, doi: 10.1109/ACCESS.2020.2968939.

[32] B. Saha and K. Goebel, "Battery data set," NASA AMES Prognostics Data Repository, Washington, DC, USA, Tech. Rep., 2007.

[33] J. Zhang and N. Tansu, "Optical gain and laser characteristics of InGaN quantum wells on ternary InGaN substrates," *IEEE Photon. J.*, vol. 5, no. 2, Apr. 2013, Art. no. 2600111.

[34] S. Azodolmolky, J. Perelló, M. Angelou, F. Agraz, L. Velasco, S. Spadaro, Y. Pointurier, A. Francescon, C. V. Saradhi, P. Kokkinos, E. Varvarigos, S. A. Zahr, M. Gagnaire, M. Gunkel, D. Klonidis, and I. Tomkos, "Experimental demonstration of an impairment aware network planning and operation tool for transparent/translucent optical networks," *J. Lightw. Technol.*, vol. 29, no. 4, pp. 439–448, Sep. 15, 2011.

[35] C. Zhang, S. Zhao, and Y. He, "An integrated method of the future capacity and RUL prediction for lithium-ion battery pack," *IEEE Trans. Veh. Technol.*, vol. 71, no. 3, pp. 2601–2613, Mar. 2022, doi: 10.1109/TVT.2021.3138959.

[36] D. Zhou, Z. Li, J. Zhu, H. Zhang, and L. Hou, "State of health monitoring and remaining useful life prediction of lithium-ion batteries based on temporal convolutional network," *IEEE Access*, vol. 8, pp. 53307–53320, 2020, doi: 10.1109/ACCESS.2020.2981261.

[37] M. U. Ali, A. Zafar, S. H. Nengroo, S. Hussain, G.-S. Park, and H.-J. Kim, "Online remaining useful life prediction for lithium-ion batteries using partial discharge data features," *Energies*, vol. 12, no. 22, p. 4366, Nov. 2019, doi: 10.3390/en12224366.

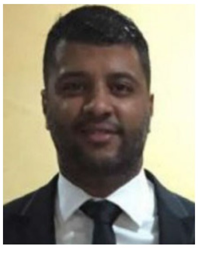

ANAS TIANE (Member, IEEE) received the M.B.A. degree from the University of Ottawa, Ottawa, ON, Canada, in 2010, the master's degree (Hons.) in computer science from the University of Quebec, Outaouais, QC, Canada, in 2012, and the Ph.D. degree in electrical and computer engineering from Carleton University, Ottawa, in 2023. He has more than 20 years of experience as an IT professional specializing in the field of big data, machine learning, and artificial intelligence.

CHAFIK OKAR (Member, IEEE) received the Ph.D. degree (Hons.) in science and technology from Abdelmalek Saadi University, Tetouan, Morocco, in 2011. From 2002 to 2011, he held various engineering and management positions with Moroccan Industry. From 2011 to 2018, he was an Assistant Professor with Hassan First University, Settat, Morocco. From 2020 to 2022, he was a Senior Postdoctoral Fellow with Carleton University, Ottawa, ON, Canada. He is currently a Logistics Professor with the National School of Applied Sciences of Tetouan, Abdelmalek Essaâdi University. His career has spanned both academia and industry in the field of data analysis and supply chain management. He authored or coauthored more than 50 journal and conference publications. His research interests include machine learning, manufacturing engineering, industrial engineering, and information science and storage systems.

MOHAMAD ALZAYED (Member, IEEE) received the Ph.D. degree in electrical and computer engineering from Carleton University, Ottawa, ON, Canada. Since 2019, he has been a member with the Intelligent Robotic and Energy Systems (IRES) Research Group, Department of Electronics, Carleton University. His career has bridged both academia and industry with more than 14 years of experience in control and electrical energy resources, grid management and efficiency, electrical design and contracting, and project management. His teaching/research interests include intelligent control of electric machines and power converters for energy systems, real-time simulations, and power systems. He is a guest editor of several journals.

HICHAM CHAOUI (Senior Member, IEEE) received the Ph.D. degree in electrical engineering from the University of Quebec, Trois-Rivières, QC, Canada, in 2011. From 2007 to 2014, he held various engineering and management positions with Canadian Industry. He is currently an Associate Professor with Carleton University, Ottawa, ON, Canada. He is a Registered Professional Engineer in the Province of Ontario. His career has spanned both academia and industry in the field of control and energy systems. His scholarly work has resulted in more than 200 journal and conference publications. He was a recipient of the Best Thesis Award, the Governor General of Canada Gold Medal Award, the Carleton's Research Excellence Award, the Early Researcher Award from the Ministry of Colleges and Universities, and the Top Editor Recognition from the IEEE Vehicular Technology Society. He is an associate editor of several IEEE journals.